Construction and Building Materials 34 (2012) 151–161

Contents lists available at SciVerse ScienceDirect

Construction and Building Materials

journal homepage: www.elsevier.com/locate/conbuildmat

Comparative assessment of load–resistance factor design of FRP-reinforced cross sections

Iunio Iervolino *, Carmine Galasso

Dipartimento di Ingegneria Strutturale, Università degli Studi di Napoli Federico II, Naples, Italy

ARTICLE INFO

Article history:
Received 1 November 2011
Received in revised form 20 February 2012
Accepted 25 February 2012

Keywords:
Fiber-reinforced polymers
Bending
Safety factors
Structural reliability
LRFD

ABSTRACT

In the last decades, codes have implemented the load–resistance factor design (LRFD) approach to achieve a certain safety level in structural sections. Recently, the same philosophy established in the case of steel bars was adapted for reinforcement by innovative materials such as fiber-reinforced polymers (FRPs). LRFD is claimed to be a semi-probabilistic approach, although the implied safety is not intelligible by practitioners, being hidden into the so-called safety factors (SFs) prescribed by codes, which should account for load- and strength-affecting heterogeneities. Often, especially in the case of FRP reinforcement, the SFs differ from one code to another because of the format of the design equations. The objective of the simple study presented in the paper is to compare the safety levels, expressed in terms of conventional probability of failure, for different codes at the state-of-the art with respect to the design of FRP-reinforced concrete worldwide. The purpose is to investigate how the different equation formats, design values of material properties, and partial safety factors, affect the implicit design safety and whether it is similar among international guidelines. The study considers design of cross sections in bending at the ultimate limit state according to: ACI 440.1R-06 (US guidelines), CAN/CSA-S806-02 (Canadian guidelines), and CNR-DT 203/2006 (Italian guidelines, for which sensitivity of design to SFs is also investigated). For comparison purposes, design of steel-reinforced sections is considered according to the recent Italian regulations. Results indicate that reliability indices achieved with design procedures are generally comparable among the considered codes, and larger than that referring to steel reinforcement.

1. Introduction

This section briefly reviews the basics of safety formats in international design codes and motivates the study. In fact, although the most of the background may be found in well-known literature (e.g., [1]), it may be worthwhile to recall the working hypotheses of current practice, as they are not directly intelligible from guidelines. At the end of the introduction, the framework of the guidelines is presented and the organization of the work is given.

The objective of structural design is that the construction warrants a given safety margin with respect to some feared *failure mode*. In fact, structural safety has to refer to an undesired condition (*limit state* hereafter), which may lead to some unacceptable situation, namely *failure*. The quantification of safety consists of the *reliability* assessment, that is, the evaluation of the *probability of safe behavior*, P_s. For any engineering system P_s has to be referred to the time in which it operates; e.g., the *design life* (T).

Structural reliability has to be necessarily expressed in probabilistic terms because most, if not all, the factors possibly determining failure are uncertain despite the values assumed in design; e.g., mechanical models, members' geometry, materials' properties, and loads. In fact, these are called random variables (RVs), $\overline{X} = \{X_1, X_2, \ldots, X_n\}$, whose actual heterogeneity is characterized by appropriate probability density functions (PDFs) for each instant in the lifetime of the structure generating, in fact, *stochastic processes* (e.g., [2]).

If the failure for the structure of interest may be expressed by a function, G, which is positive if the system is in safe conditions and is non-positive if limit state of interest is reached, for example, in the *stress–strength* model, the difference between the *resistance* (R) and its counterparts due to *loads* (L), the structural reliability may be expressed as the probability that the limit state function remains positive in the $(0, T)$ interval (being 0 the life's start time), Eq. (1), from which the probability of failure[1] (P_f) emerges.

$$P_s(T) = 1 - P_f(T) = \Pr[G(\overline{X}, t) > 0 \; \forall t \in (0, T)] = \Pr[R(\overline{X}, t) - L(\overline{X}, t) > 0 \; \forall \, t \in (0, T)] \quad (1)$$

* Corresponding author. Address: Dipartimento di Ingegneria Strutturale, Università degli Studi di Napoli Federico II, Via Claudio 21, 80125 Naples, Italy. Tel.: +39 0817683488; fax: +39 0817685921.
E-mail address: iunio.iervolino@unina.it (I. Iervolino).

[1] Because, it is expected the reliability of structures to be high (e.g., P_s is relatively close to 1) may be handy to work in terms of P_f expressed as a power of ten.

0950-0618/$ - see front matter © 2012 Elsevier Ltd. All rights reserved.
http://dx.doi.org/10.1016/j.conbuildmat.2012.02.021

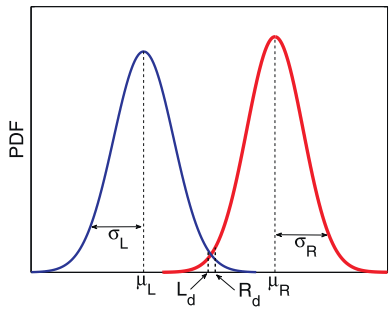

Fig. 1. *Stress–strength* model for reliability assessment. For simplicity Gaussian PDF shape is considered for both PDFs of R and L.

Calibrating the RVs in a way that their variability does not explicitly depend on time anymore (i.e., rendering the safety assessment a *time-invariant* problem; e.g., [3]) the failure probability is expressed by the integral of the joint PDF of the variables, $f_{\overline{X}}(x_1, x_2, \ldots, x_n)$, over the domain in which the set of $\overline{X}$ renders G non positive (i.e., the *failure domain* or F), as follows:

$$P_f = \Pr[\overline{X} \in F] = \int_{F:G\leqslant 0} f_{\overline{X}}(x_1, x_2, \ldots, x_n) \cdot dx_1 \cdot dx_2 \ldots dx_n \quad (2)$$

A reliability-oriented structural code should ask the practitioner to assess the safety of a structure (either of new design or existing) computing the probability of failure and verifying whether it does not exceed some upper bound that is considered acceptable (P_f^*), as follows:

$$P_f \leqslant P_f^* \quad (3)$$

Modern codes do not allow for such an explicit approach for various reasons, mostly related to the difficulty of giving practice-ready procedures to assess the probability of failure, and the persistent need to have a prescriptive format of design rules. In fact, Eq. (3) is replaced by one of the type of Eq. (4), which basically is a comparison of *design* values of actions due to loads (L_d) and resistance (R_d) computed via deterministic equations, which are familiar to engineers.

$$L_d \leqslant R_d \quad (4)$$

This is done at a sectional level, while it should be more correctly computed for the whole structure; however, that would imply significant complications. Leaving the probabilistic approach to a sectional level inevitably renders the failure probabilities conventional, in a way that they do not represent failure probability of structures where such sections are employed and usable for comparison purposes only [4].

If the terms in Eq. (4) are calibrated based on the PDFs of L and R (separately if stochastically independent) this approach is considered *semi-probabilistic* and referred to as *load–resistance factor design* (LFRD); [5]. In fact, L_d and R_d reflect the probabilistic nature of L and R through some coefficients called safety factors (SFs) and applied, depending on the code, to statistics of uncertain design variables affecting R and L, or directly on measures of resistance and loads effects acting on the structural element (to follow).

When postulated, about four decades ago, LFRD was conceived to be *temporary*. It was supposed to be shortly replaced by codes allowing professionals to compute Eq. (2) explicitly for their structures [6]. Nevertheless, it is still used around the world and also adopted by regulations concerning new technologies in civil engineering, such as reinforced concrete (RC) structures employing fiber reinforced polymers (FRPs). This is mainly because its afore mentioned probabilistic basis and simplicity of application by reliability non-experts. However, codes seldom clearly report the calibration of the design parameters and the underlying hypotheses, and, therefore, safety implied in design is not directly intelligible. Moreover, design equations are custom for each code and it is also not possible to compare them in terms of implicit safety. This motivated other work (e.g., [7–9]) and the simple investigation presented in the following, where a probabilistic assessment for international codes dealing with FRP-RC cross sections is carried out. In fact, the purposes of this study may be summarized as: (i) to understand how the format of design equations, material properties assumed for computations, and safety factors (eventually partial), affect safety of cross sections at ultimate limit state in each guideline; and (ii) to address whether the different declensions of LRFD in each code imply comparable safety.

In particular, reliability analysis of flexural capacity of glass fiber-reinforced polymer (GFRP) RC cross sections at *ultimate limit state* (ULS) is performed. The analysis considers design of cross sections in bending according to three codes: ACI 440.1R-06 (*US guidelines*; [10]), CAN/CSA-S806-02 (*Canadian guidelines*; [11]), and the *Italian guidelines* CNR-DT 203/2006 [12]. For comparison, design of steel-reinforced sections according to the recent new Italian Building Code or NIBC [13] is also included. These three codes were chosen to cover the majority of modern standards concerning design of concrete reinforced with composite materials.

Case studies concern design of cross sections, according to the codes, for different values of the safety factors. Subsequently, conventional failure probability is computed and compared. Finally, for CNR-DT 203/2006, it is analyzed how sensitive is design to different SF values.

2. Basics of load–resistance factor design

Typical categories of uncertainty in structural analysis are loads, material strengths, member geometries, and there is also some uncertainty related to the mechanical (analytical) models assumed (e.g., [1,14]). If a cross section in bending is considered, uncertainty

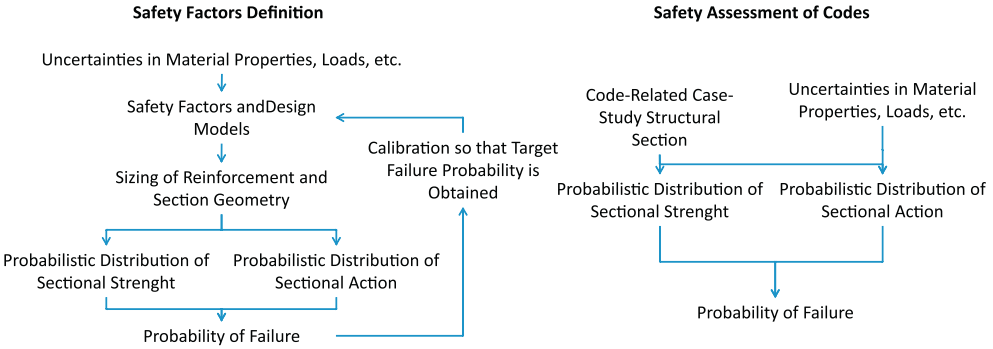

Fig. 2. Calibration of safety factors (left), and safety assessment procedure (right).

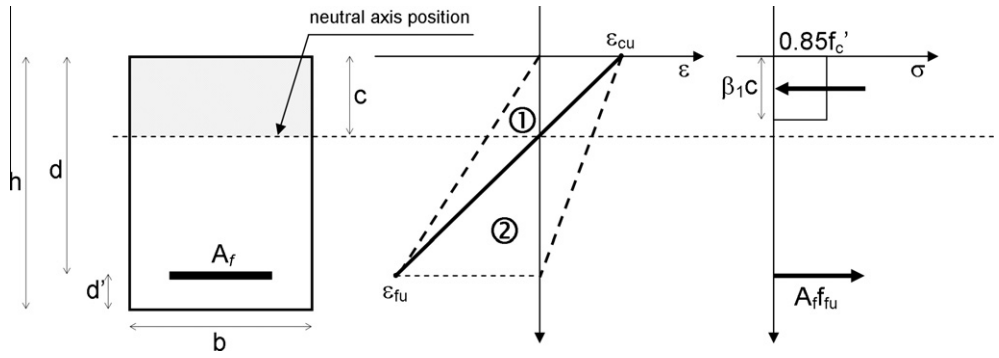

Fig. 3. Sketch for analysis of FRP-RC cross section.

is reflected in both soliciting and resisting moments, and if is it possible to characterize mathematically this lack of knowledge by appropriate PDFs, safety may be quantitatively evaluated. Roughly speaking, if the mean, μ, of R is larger than that of L, then the probability of failure is directly proportional to the separation between the two PDFs (considered stochastically independent). In fact, smaller is the overlapping area, safer is the cross section, as in Fig. 1. Given this concept, the original version of LRFD approach relies on a prescribed factor (the *central safety factor*, ϕ_0, larger than one; [5]) which is the ratio of R and L expectations, as follows:

$$\mu_R \geqslant \phi_0 \cdot \mu_L \tag{5}$$

In other words, if the cross section is designed so that the average strength is ϕ_0 times the average load effect, a certain "distance" between R and L PDFs is assured in a way that, given the dispersions or standard deviations (σ, roughly speaking: a measures how flat the PDFs are if Gaussian shape is assumed), an acceptable failure probability is obtained. In fact, ϕ_0 acts as a way to oversize the section to assure a large expected strength, as shown in Fig. 2, left.

Alternate, although equivalent, formats of LRFD exist, in which the safety factor (ϕ) is not the central one, being applied to percentiles of the distributions of R (r_k) and L (l_k), Eq. (6). However, because the percentiles are functionally related to some parameters of the PDF, for example they may be a few (α-times) standard deviations (σ) away from the mean as in Eq. (7); this format is equivalent to Eq. (5)

$$r_k \geqslant \phi \cdot l_k \tag{6}$$

$$\begin{cases} r_k = \mu_R - \alpha_R \cdot \sigma_R \\ l_k = \mu_L + \alpha_L \cdot \sigma_L \end{cases} \tag{7}$$

In codes, generally, R_d and L_d are obtained using separate factors reducing strength (ϕ) and amplifying load effects (γ); i.e., Eq. (8).

$$R_d = \frac{r_k}{\phi} \geqslant \gamma \cdot l_k = L_d \tag{8}$$

Other codes do not apply safety factors to the sectional strength; instead they reduce the material's ultimate resistance using conservative percentiles as design values. This makes the obtained sectional strength a conservative percentile of the PDF of R. Design values are obtained by applying SFs to some percentiles obtained by material testing (for concrete and reinforcement, for example, $f_{u,c}$ and $f_{u,r}$, respectively) leading to Eq. (9), in which sectional strength is function of SFs applied to materials.[2]

$$R_d = R\left(\frac{f_{u,c}}{\phi_c}, \frac{f_{u,r}}{\phi_r}\right) \geqslant \gamma \cdot l_k = L_d \tag{9}$$

[2] In the following separate safety factors will also be assumed for dead and live loads.

To assess the safety level implied by codes, at least at a sectional level, one should design representative case studies applying the safety factors specified for materials and loads, and reproduce the PDFs of the action and strength for the designed sections. This allows the computation of failure probability as a function of the safety factors (Fig. 2, right), and it is the approach followed in the study focusing only on the safety factors to be applied on nominal resistance/material properties as provided by each considered code.

3. Design of FRP-reinforced concrete

Fiber reinforced polymers are impacting the international concrete industry; they can be used as both internal and external reinforcement for structural members providing an effective and cost-efficient alternative to reinforcing steel, especially in corroding environment (e.g., [15]). Extensive research has supported the FRP application in civil engineering and has provided the current confidence to use it in practice (e.g., [16,17]). However, there are a limited number of standards and codes that address design of FRP-reinforced concrete; examples are in United States, Canada, Japan, and, more recently, Italy.

Design of FRP-RC members for flexure is analogous to the design of steel-RC members, being based on similar assumptions. However, the modulus of elasticity of FRP is much lower than that of steel and thus, larger strains are needed to develop comparable tensile stresses in the reinforcement. In fact, given comparable strength of two sections reinforced with FRP and steel, the former should have larger deflections and crack widths with respect to the latter. This is why serviceability limit states may control design. Moreover, design procedures account for brittle behavior of both FRP and concrete. Therefore, while steel-reinforced sections are explicitly designed to have a ductile failure in ultimate conditions, FRP-reinforced concrete sections cannot display the same energy dissipation capacity. Based on these considerations, the concrete may be *over-reinforced* [17]; if the section fails, the concrete will crush (i.e., compression-controlled failure) providing some warning of failure. If the amount of reinforcement is such that failure is tension-controlled, that is FRP fails, collapse may me brittle. However, in such a case there may be some warning of impending failure, because of extensive cracking and large deflections due to the FRP elongation.

In the following, ULS design according to different codes is reviewed. The US design approach is based on the inequality of Eq. (10), similar to Eq. (8), in which R_n is the nominal strength of member (in terms of bending moment), ϕ is the *strength reduction factor* (lower than one in this case), and L_d is the design load effect

$$\phi \cdot R_n \geqslant L_d \tag{10}$$

The Italian (European, actually) and Canadian approaches are based on Eq. (9) in which R_d is the design value of the ultimate member resistance, computed as a function of the design strength

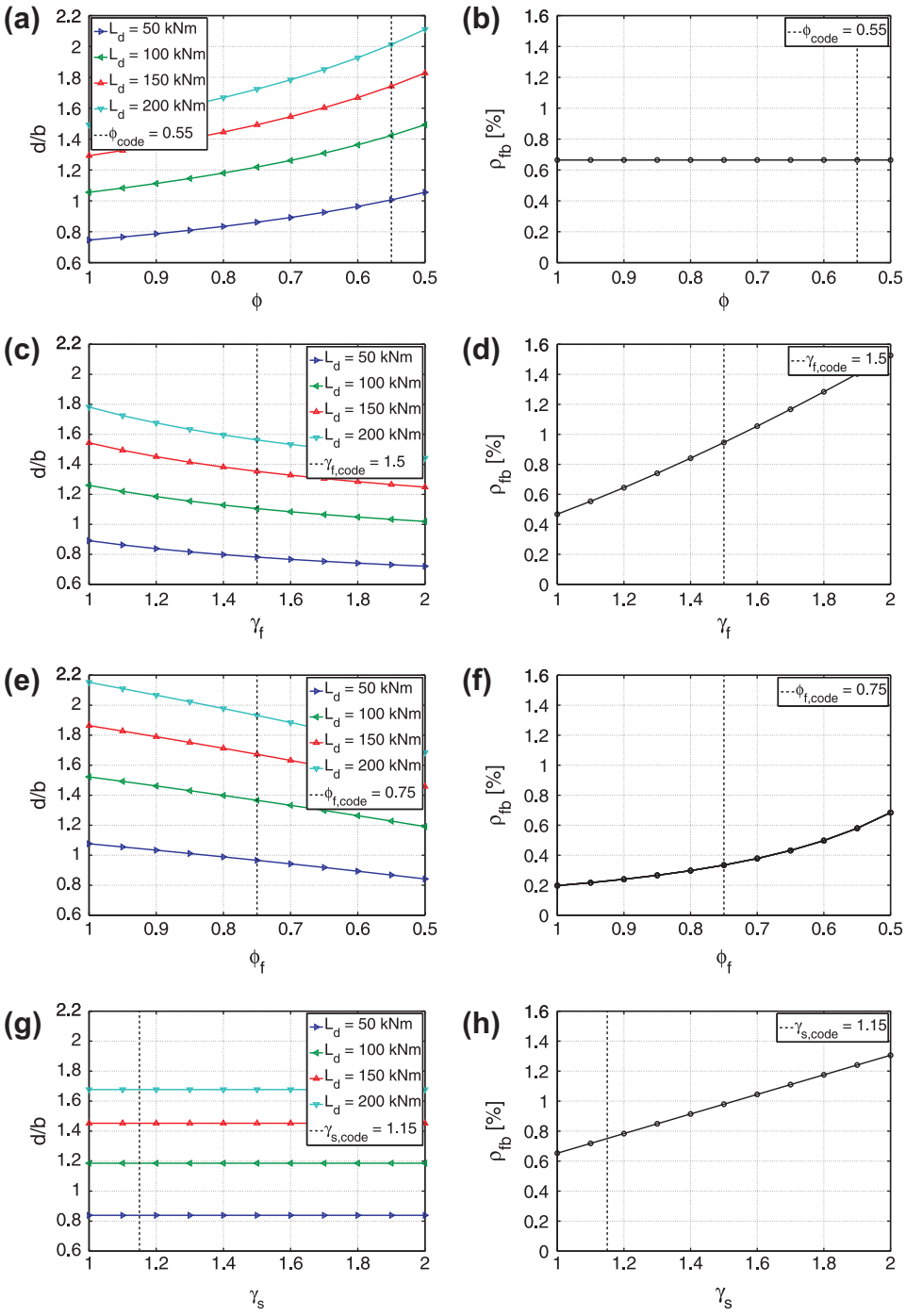

Fig. 4. Trends of effective height on width ratio and reinforcement ratio for balanced failure condition as function of codes safety factors, for different values of the factored moments. (a) and (b) US guidelines, (c) and (d) Italian guidelines, (e) and (f) Canadian guidelines, and (g) and (h) steel reinforced concrete sections.

of materials (derived dividing the characteristic material strength by material safety factor, see next section) and L_d is the design load effect also, based on percentiles.

3.1. US guidelines

In the US, design of concrete structures reinforced with FRP bars is based on documents produced by American Concrete Institute (ACI) – Committee 440. ACI design guidelines for structural RC with FRP bars (ACI 440.1R-06 [10]) are primarily based on modifications of ACI-318 (ACI 318-05 [18]); i.e., the standard building code requirements for structural concrete (reinforced with steel bars). In ACI guidelines the sectional design flexural strength, which is the nominal flexural strength of the member, M_n, multiplied by a strength reduction factor, ϕ (this product gives R_d), has to exceed the factored moment (referred to as *required strength* in ACI 318-05) M_u (i.e., L_d), as follows:

$$\phi \cdot M_n \geqslant M_u \tag{11}$$

According to ACI guidelines both concrete crushing and FRP rupture are acceptable failure modes, although concrete crushing is preferred. The failure mode can be determined by comparing

Table 1
Case study cross sections.

Code	Failure mode	d (mm)	A_f (mm^2)	$\frac{\rho}{\rho_{fb}}$	R_d (kNm)
ACI	Concrete	370	1104	1.50	104
	GFRP	600	614	0.50	101
CNR	Concrete	310	1350	1.50	101
	GFRP	460	736	0.50	109
CAN	Concrete	380	614	1.50	104
NIBC (steel)	Concrete	360	859	1.00	108

the FRP reinforcement ratio, ρ_f, Eq. (12), to the balanced reinforcement ratio, ρ_{fb}, which is the ratio where concrete crushing and FRP rupture occur simultaneously, as follows:

$$\rho_f = \frac{A_f}{b \cdot d} \tag{12}$$

$$\rho_{fb} = 0.85 \cdot \beta_1 \cdot \frac{f'_c}{f_{fu}} \cdot \frac{E_f \cdot \varepsilon_{cu}}{E_f \cdot \varepsilon_{cu} + f_{fu}} \tag{13}$$

In Eqs. (12) and (13): A_f is the FRP area, b and d are width and effective depth of the section (Fig. 3); β_1 is a *stress-block* factor for concrete depending on material properties (taken as 0.85 for concrete strength, f'_c, up to and including 28 MPa; for strength above 28 MPa, this factor is reduced continuously at a rate of 0.05 per 7 MPa of strength in excess of 28 MPa, but is not taken less than 0.65); f'_c is the compressive strength of concrete evaluated on cylindrical specimens; E_f is the warranted modulus of elasticity of FRP; f_{fu} is the design tensile strength of FRP and ε_{cu} is the ultimate compressive strain of concrete (equal to 0.003).

The design tensile strength, f_{fu}, may be determined by Eq. (14) where C_E is an environmental reduction factor depending on the fiber type and exposure conditions (equal to 0.7 for GFRP bars and concrete exposed to earth and weather, as considered in this paper), f^*_{fu} is the *manufacturer-guaranteed* tensile strength of FRP bars, defined as the mean tensile strength of a sample of test specimens ($f_{fu,ave}$) minus three standard deviations (σ), Eq. (15). This guaranteed strength provides a 99.87% probability that similar FRP bars exceed the indicated value. Depending on the number of tested specimens, the confidence level of the distribution parameters and then, of the guaranteed tensile strength, may be determined. The design rupture strain should be determined similarly.

$$f_{fu} = C_E \cdot f^*_{fu} \tag{14}$$

$$f^*_{fu} = f_{fu,ave} - 3 \cdot \sigma \tag{15}$$

If $\rho_f \leqslant \rho_{fb}$, FRP failure determines the nominal flexural strength, M_n, which may be computed via the simplified and conservative formula in Eq. (16); otherwise concrete crushing is the failure mode to consider and Eq. (17), based on stress-block approach, applies

$$M_n = A_f \cdot f_{fu} \cdot \left(d - \frac{\beta_1 \cdot c_b}{2}\right) \tag{16}$$

$$M_n = \rho_f \cdot f_f \cdot \left(1 - 0.59 \cdot \frac{\rho_f \cdot f_f}{f'_c}\right) \cdot b \cdot d^2 \tag{17}$$

In Eq. (16), $c_b = \left(\frac{\varepsilon_{cu}}{\varepsilon_{cu}+\varepsilon_{fu}}\right) \cdot d$ is the neutral axis depth when both materials are at ultimate deformation (i.e., *balanced-failure* condition); in Eq. (17), $f_f = \left(\sqrt{\frac{(E_f \cdot \varepsilon_{cu})^2}{4} + \frac{0.85 \cdot \beta_1 \cdot f'_c}{\rho_f} \cdot E_f \cdot \varepsilon_{cu}} - 0.5 \cdot E_f \cdot \varepsilon_{cu}\right) \leqslant f_{fu}$. In FRP-failing sections, the actual depth of neutral axis (c in Fig. 3) is lower than c_b leading to a greater value of M_n.

The strength reduction factor ϕ assigned by the code is given in Eq. (18) and is equal to 0.65 in case of concrete crushing, 0.55 for FRP rupture, and varies linearly between the two. Eq. (18) implies that a section is controlled by concrete crushing if the reinforcement ratio, ρ_f, is equal or larger than 1.4 times the ρ_{fb}. While concrete crushing failure mode can be predicted based on calculations, the member as constructed may not fail accordingly. For example, if the concrete strength is higher than specified, the member can fail due to FRP rupture. For this reason, and to establish a transition between the two values of ϕ, a section controlled by concrete crushing is defined as a section in which $\rho_f \geqslant 1.4 \cdot \rho_{fb}$

$$\phi = \begin{cases} 0.55 & \rho_f \leqslant \rho_{fb} \\ 0.3 + 0.25 \cdot \frac{\rho_f}{\rho_{fb}} & \rho_{fb} < \rho_f < 1.4 \cdot \rho_{fb} \\ 0.65 & \rho_f \geqslant 1.4 \cdot \rho_{fb} \end{cases} \tag{18}$$

3.2. Italian guidelines

Italian design guidelines [12], *Guidelines for the Design and Construction of Concrete Structures Reinforced with Fiber-Reinforced Polymer Bars*, have been developed within the framework of the Italian Consiglio Nazionale delle Ricerche (CNR). The new document adds to the series of documents recently issued by CNR on the structural use of fiber reinforced polymer composites, starting with the publication of CNR-DT 200/2004 [19], pertaining to the use of externally bonded systems for strengthening concrete and masonry structures.

According to Italian guidelines, flexural design at ULS requires that the design ultimate moment M_{Sd} (i.e., the design load effect, L_d) and the design flexural capacity M_{Rd} (i.e., the design value of resistance, R_d) of the FRP-RC element to satisfy as follows:

$$M_{Sd} \leqslant M_{Rd} \tag{19}$$

Referring to Fig. 3, it is assumed that failure occurs when one the following conditions is met:

1. the maximum concrete compressive strain ε_{cu} (equal to 0.0035) is reached, while the ultimate strain of FRP has not been attained yet;
2. the maximum FRP tensile strain ε_{fd} is reached. ε_{fd} is computed from the characteristic tensile strain (i.e., having a 95% probability of exceedance according to material specifications), ε_{fk}, as in Eq. (20).

$$\varepsilon_{fd} = 0.9 \cdot \eta_a \cdot \frac{\varepsilon_{fk}}{\gamma_f} \tag{20}$$

The coefficient 0.9 in Eq. (20) accounts for the lower ultimate strain of bars embedded in specimens subjected to bending as compared to bars subjected to standard uniaxial tensile tests; η_a is an environmental factor (it is analogous to C_E in ACI guidelines) also depending on the fiber type (for concrete exposed to moisture and reinforced with GFRP bars $\eta_a = 0.7$); γ_f is the material *partial safety factor* equal to 1.5 for ULS, analogous to ϕ_r in Eq. (9).

Design flexural capacity, M_{Rd}, can be determined based on strain compatibility, internal forces equilibrium and the controlling mode of failure. According to the current NIBC (to which CNR refers), design at ULS can assume a simplified distribution of the normal stress for concrete (i.e., stress-block) for elements whose failure is initiated either by crushing of concrete or rupture of FRP bars, leading to design equations similar to Eqs. (16) and (17), provided that design values of materials strength are used (i.e., fifth percentile values divided by the material safety factors, and amplified by 0.9 times η_a in the case of GFRP). The partial safety factor $\gamma_c = 1.5$ prescribed by the NIBC shall be assigned to concrete; analogous to ϕ_c in Eq. (9).

3.3. Canadian guidelines

The Canadian Standard Association (CSA) design guidelines CAN/CSA-S806-02 [11] were approved in 2004 as a national standard. The approach is similar to the Italian one and it considers *partial* safety factors applied to materials to get a conservative sectional strength. However, all FRP reinforced concrete sections shall be designed in such a way that failure of the section is initiated by crushing of concrete; i.e., tensile fracture of the reinforcement is not allowed.

The design tensile strength of FRP bars, f_{fu}, may be determined by Eq. (21) where ϕ_f is the strength reduction factor of FRP rod and it is depending on the fiber type, f^*_{fu} is the manufacturer-warranted tensile strength of an FRP bar and it must have 95% probability of exceedance (i.e., 5th percentile of material strength distribution). The partial factor ϕ_f is equal to 0.75 for GFRP reinforcement. The strength reduction factor of concrete, ϕ_c, is equal to 0.65.

$$f_{fu} = \phi_f \cdot f^*_{fu} \tag{21}$$

4. Design of case studies

In order to introduce the case studies analyzed in the following, in Fig. 4 parametric examples of design according to the considered codes are given. In particular, the trends of the balanced $\frac{d}{b}$ ratio and the balanced reinforcement ratio, ρ_{fb}, as a function of ϕ for the US guidelines (Fig. 4a and b), γ_f for the Italian guidelines (Fig. 4c and d), and ϕ_f for the Canadian guidelines (Fig. 4e and f), are reported for four different values of design bending moment, L_d; i.e. 50, 100, 150 and 200 kNm. For comparison, design of steel-reinforced sections according to NIBC is also reported in Fig. 4g and h.

In designing the sections, based on equilibrium equations, material properties (in terms of ultimate strains and strengths) were selected a priori, leaving the area of longitudinal reinforcement A_f (and consequently ρ_{fb}), and the effective depth, d, as the design variables. More specifically: b was assumed equal to 300 mm, concrete characteristic cylindrical compressive strength (hereafter, the term *characteristic* refers to values of material properties having a 95% probability of exceedance according to material specifications) equal to 25 MPa, GFRP characteristic strength equal to 916 MPa (a guaranteed tensile strength of 855 MPa according to ACI guidelines), GFRP characteristic tensile rupture strain equal to 1.9% (a guaranteed rupture strain of 1.8% according to ACI guidelines), and a GFRP modulus of elasticity equal to 46 GPa (see [20] for further details). Reinforcing steel characterized by a characteristic yield stress of 450 MPa (B450C reinforcing bars, according to NIBC) was considered (the balanced failure for steel RC is based on an steel ultimate strain equal to 1%[3]; the actual–experimental–steel ultimate strain is much larger, even by one order of magnitude) leading to cross section characterized always by concrete crushing. L_d was assumed equal to R_d, which is $\phi \cdot M_n$ in the case of ACI, and M_{Rd} in the case of Italian and Canadian guidelines. The balanced reinforcement ratio is influenced by both strength and tensile ultimate strain of GFRP; it varies between 0.5% and 1.5% when γ_f varies between 1 and 2 (Italian guidelines), between 0.7% and 0.2% when ϕ_f varies between 0.5 and 1 (CAN guidelines). According to ACI guidelines, ρ_{fb} is independent on ϕ, Eq. (13).

Fig. 4h indicates that, in the case of steel reinforcing bars, the balanced reinforcement ratio is linearly dependent on γ_s as the conventional ultimate deformation assumed for steel is independent on γ_s and, then, only the material strength (dependent on γ_s) affects ρ_{fb}. Fig. 4g indicates that, in the case of steel reinforcing bars, the balanced $\frac{d}{b}$ ratio is constant as the conventional tensile ultimate strain assumed for steel is independent on γ_s. In the case of ACI, the safety factor acts directly on the factored moment increasing it, and then the cross-section geometry increases. Both CNR and CAN apply the SF to the materials' property, reducing the GFRP ultimate strain, the design results in larger value of the reinforcement area in smaller cross-section dimensions.

In order to compare the safety levels implicit to the analyzed codes, six case study sections were designed assuming a value of the design moment L_d equal to 100 kNm and with one layer of reinforcement in tension. Both possible failure modes were considered in design according to ACI and CNR guidelines; for CAN guidelines, the cross section was designed in such a way that failure of the section is initiated by crushing of concrete. Sections are reinforced by GFRP bars with a diameter of 12.5 mm (i.e., the effect of discrete bar size was explicitly considered), and the same values described above were used for the width of sections and material strengths. Table 1 lists the geometrical properties for all case study cross section and the corresponding value of bending moment capacity, R_d.

Although this study aims at determining the structural reliability implied by flexural strength equations, it was mentioned in Section 3, that serviceability limit states, such as crack-width, may control design of FRP reinforced concrete. Therefore, it was verified the case-study cross sections satisfy the serviceability limit states checks according to the considered codes.

For comparison, design of steel-reinforced sections according to the recent Italian code is also considered in Table 1. Reinforcing steel is characterized by a specified yield stress of 450 MPa (as discussed above) and a steel partial safety factor equal to 1.15 is assumed. An elastic-perfectly-plastic stress–strain diagram for steel with 7% ultimate strain warrants the failure of the section always occurs due to concrete crushing, therefore case study refers to just one failure mode.

As shown in Table 1, given the strength, for the sections experiencing GFRP bars' failure, the dimensions are larger (about 60% in the case of ACI guidelines and about 50% in the case of CNR guidelines) with respect to the case when concrete is crushing (in this latter case, the geometry of the cross sections is almost the same

Table 2
Summary of resistance and load statistics and distribution models.

Category	Variable	Bias	CoV (%)	Distribution
Material	Concrete strength (f_c)	1.05	10	Normal
	GFRP strength (f_r)	1.20	7	Normal
	Steel strength (f_y)	1.10	5	Normal
Load	Dead load (M_D)	1.05	10	Normal
	Live load (M_L)	1.00	25	Gumbel
Geometry	Width of beam (b)	1.10	4	Normal
	Effective depth of beam (d)	0.99	4	Normal
	Reinforcement area (A_f)	1.00	5	Normal
Model	Concrete crushing (GFRP reinforcement)	1.10	9	Normal
	Concrete crushing (steel reinforcement)	1.01	10	Normal
	GFRP fracture	1.11	9.5	Normal

Table 3
Basic load partial factors.

Code	γ_L	γ_D
ACI	1.6	1.2
CNR, NIBC	1.5	1.3
CAN	1.5	1.25

[3] In this way, the reinforcement yields well before the concrete crushes.

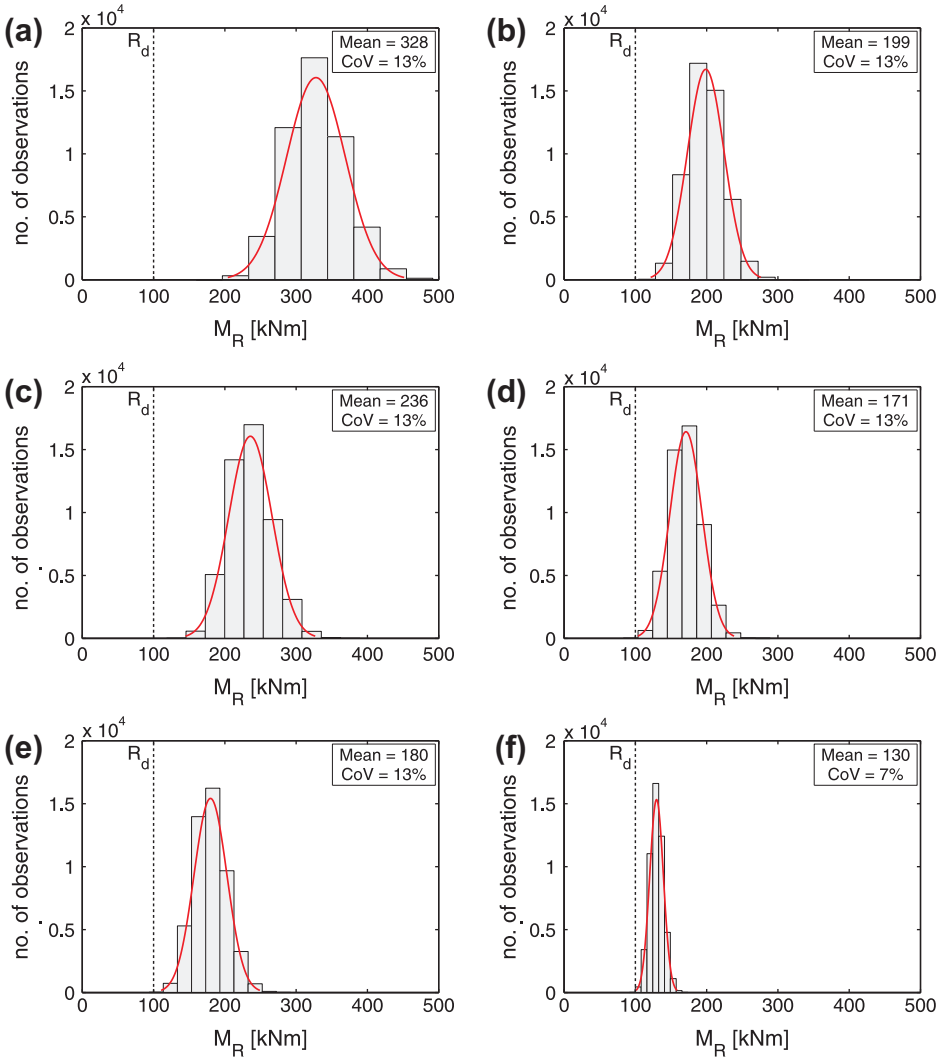

Fig. 5. Distribution of M_R obtained using Montecarlo simulation and superimposed normal PDFs. (a) ACI guidelines, GFRP fracture; (b) ACI guidelines, concrete crushing; (c) CNR guidelines, GFRP fracture; (d) CNR guidelines, concrete crushing; (e) CAN guidelines, concrete crushing (f) NIBC (steel), concrete crushing.

across the considered guidelines). For ACI guidelines, this larger difference in the concrete geometry is due to the strong reduction of the nominal flexural strength when GFRP bars' rupture occurs, Eq. (18), and to the lower percentile used in defining the nominal strength of GFRP bars with respect to CNR guidelines, Eq. (15).

In the case of the CAN guidelines, the absence of an environmental factor and the smaller value of the safety factor for GFRP strength, lead to a larger value of the nominal strength of GFRP bars and, then, to a reinforcement area smaller with respect to concrete crushing in the other codes. The same conclusion holds for the steel-reinforced concrete due to the smaller value of the partial safety factor used for steel; however, with respect to the Canadian guidelines, the area of steel reinforcement is larger because the conventional value for steel tensile design ultimate strain is equal to 1% (less than the design ultimate strain for GFRP bars).

5. Uncertainty characterization

A literature review was carried out to select the statistical characterization for each RV referring to materials, loads, geometry and models. The resulting assumptions are summarized in Table 2 and described in the following sub-sections. All RVs were considered as stochastically independent.

5.1. Materials

Statistical properties of concrete and steel are comprehensively documented in [14,21]. The parameters given in Table 2 are the bias (the ratio between the mean of a random variable and the nominal value), and the coefficient of variation (CoV) defined as the ratio of the standard deviation to the mean.

The random variables describing the compressive strength of concrete, f_c, and the yielding stress of steel, f_y, are assumed to be normally distributed. Also the random variable describing the tensile strength of GFRP reinforcement, f_r (f_{fu} defined above, represents a given percentile of its PDF), is assumed to follow the normal model.[4] This assumption is well established in literature and in codes (e.g., in ACI guidelines) and has been verified experimentally through tests of composite specimens with different size and nominal strength.

GFRP data are from [20]. The modulus of elasticity of GFRP, E_f, is taken as deterministic. Strength changes of concrete and GFRP due to aging and/or creep were ignored.

[4] It is to note that also the Weibull distribution is also often used to describe the strength of FRP composites (e.g., [22]).

Table 4
Summary of statistics for M_S.

Code	L_n/D_n	Mean (kNm)	Bias	CoV
ACI	0.5	77.50	0.78	0.11
	1.0	73.21	0.73	0.13
	1.5	70.83	0.71	0.15
	2.0	69.32	0.69	0.17
	2.5	68.27	0.68	0.18
CNR, NIBC	0.5	75.66	0.76	0.11
	1.0	73.17	0.73	0.13
	1.5	71.80	0.72	0.15
	2.0	70.94	0.71	0.17
	2.5	70.33	0.70	0.18
CAN	0.5	77.51	0.78	0.10
	1.0	74.58	0.75	0.13
	1.5	72.88	0.73	0.15
	2.0	71.71	0.72	0.17
	2.5	71.05	0.71	0.18

5.2. Loads

The combination of dead and live loads, as in Eq. (22), was considered to determine sectional bending design demand

$$\gamma_L \cdot L_n + \gamma_D \cdot D_n = L_d \tag{22}$$

In Eq. (22), L_n and D_n are the nominal values of load effects, in terms of bending moments, caused by live and dead loads, respectively. Since the focus of this paper is on the resistance aspects of the flexural ultimate limit state, the only load combination that is treated is that which involves dead and occupancy live loads. Table 3 lists basic load partial factors (γ_L for live load and γ_D for the dead load) in the considered codes for ULS.

The RV describing the dead load (i.e., the gravity load due to the self-weight of the structure), M_D, is usually considered as a normally distributed. Ellingwood et al. [14] suggest a bias of 1.05 and a CoV of 10%. For the random variable describing live loads, M_L, a Gumbel-type [23] distribution was chosen, bias is equal to 1.0 and the CoV is 25%.

5.3. Sectional geometry

Geometry uncertainties account for the heterogeneity in dimensions of the considered structural element due to construction quality. The considered statistical parameters are still based on [14]. In particular, for the dimensions of concrete beams in bending, the bias factor was assumed equal to 1.01 for the width with a CoV of 4%, and equal to 0.99 for the effective depth with a CoV of 4%. Normal model was assumed.

For GFRP reinforcing bars, the bias factor of dimensions was selected as 1.0 with a coefficient of variation equal to 5% in a Normal model.

5.4. Mechanical models

Model uncertainties characterize heterogeneity in sectional capacity estimation due to design equations. In fact, they are generally measured comparing the flexural capacity obtained in experimental tests with the corresponding values obtained via analytical formulations. Statistical properties of models are comprehensively documented in [14] for steel reinforcement and in [9] for FRP reinforced concrete (the referenced study addresses reliability analysis of beams reinforced with GFRP). In particular, the mean value for the ratio of the test-to-predicted flexural strength for FRP-failing beams was 1.11 with a 9.5% CoV, while a bias of 1.01 with a 9% CoV was used in the concrete crushing case.

6. Methodology

Montecarlo sampling procedure was applied as the first step to accomplish the reliability assessment for the case studies, which consisted of estimating the probability of the limit state function of Eq. (23) being non-positive

$$G = M_R - (M_D + M_L) = M_R - M_S \tag{23}$$

In Eq. (23), M_R is the random variable describing the bending capacity for each case study of Table 1; M_D and M_L are the random variables describing load effects caused by dead and live loads, respectively (as discussed in the previous section) whose summation gives the total acting bending moment M_S.

Eq. (23) allows to introduce the *reliability index*, as described in Eq. (24), in which μ_G and σ_G are the mean and standard deviation of G. β, to be not confused with the stress-block factor β_1 discussed in preceding section, is a common measure of reliability because it is proportional to the distance of the mean of R and L, and inversely proportional to the combined standard deviation; i.e., it is related the overlapping area in Fig. 1. Moreover, if G has a marginal Normal distribution it is linked to the probability of failure via the Gauss function Φ; in fact, it is possible to show that P_f is equal to $\Phi(-\beta)$ which means there's a negative exponential relationship between the reliability index and the failure probability, Eq. (24).

$$P_f = \Phi\left(-\frac{\mu_R - \mu_S}{\sqrt{\sigma_R^2 + \sigma_S^2}}\right) = \Phi\left(-\frac{\mu_G}{\sigma_G}\right) = \Phi(-\beta) \tag{24}$$

In the case G has not a Normal distribution, P_f has to be computed in some other way, as Eq. (24) does not hold. To this aim, herein, 5×10^4 of random samples for M_R were generated for each design case. Then, the definition of the analytical model that better fits the flexural capacity, M_R has been investigated by studying the statistical distribution obtained using the Montecarlo simulations (Fig. 5). It was possible to conclude that the Gaussian distribution (e.g., [24]) is appropriate, as also confirmed via a Kolmogorov–Smirnov test [25] with a 5% significance level (someone would, more appropriately say, 95% significance level). Statistics for M_R are reported in Fig. 5. M_S, the statistics of which as a function of L_n/D_n ratio are reported in Table 4, is the sum of a Gumbel and Normal distributions and it may be hardly approximated by a Gaussian PDF. In fact, Fig. 6a–e show an example of plot of M_L and M_D distributions assuming a value of the design load L_d equal to 100 kNm (the same value used in the design of the case studies cross sections) and the load partial factors of Table 3 in ACI guidelines. It can be visually appreciated by Fig. 6f, for one L_n/D_n value (i.e., 0.5), that the Gaussian badly approximates M_S, especially, in the right tail. The latter is important with respect to the failure probability, and even apparently small misfits in this region may result in significant differences in P_f (to follow).

Therefore, because G does not have a Gaussian distribution, the probability of failure for each case study, are computed numerically as in Eq. (25), an application of the total probability theorem, where $F_R(s)$ and $f_S(s)$ are the cumulative distribution function (CDF) of M_R and the PDF of M_S, respectively[5] (e.g., [3]).

$$P_f = \int_{-\infty}^{\infty} F_R(s) \cdot f_S(s) \cdot ds \tag{25}$$

7. Results and discussions

As discussed in the previous section, Montecarlo simulation combined with the numerical integration of Eq. (25), was applied to calculate the failure probability for the designed cross sections for five different load effect ratios; i.e., $L_n/D_n = 0.5$, 1, 1.5, 2 and 2.5. Although G does not have a Gaussian distribution, the failure probabilities were be converted to reliability indices ($\beta = -\Phi^{-1}(P_f)$), as this is a common way of comparing safety levels. These are reported in Fig. 7 as a function of L_n/D_n, together with the relationship between β and P_f, for readability. It is possible to infer from the results that GFRP reliability indices are generally comparable and higher than those referring to steel.

It is important to note that the probability of failure computed considering normal distribution of for G (that is, for M_S), may be very different than those computed without (i.e., herein) such strong assumption because of the different shape of the tail, which at scale of small probabilities that are relevant for structural engineering applications, may significantly affect the reliability

[5] From a practical point of view, computations have been performed subtracting the distribution of soliciting moment due to dead loads to the resisting moment, i.e., M_R–M_D, the difference of which is still Gaussian, and considering the distribution of the soliciting moment as Gumbel distributed, M_L.

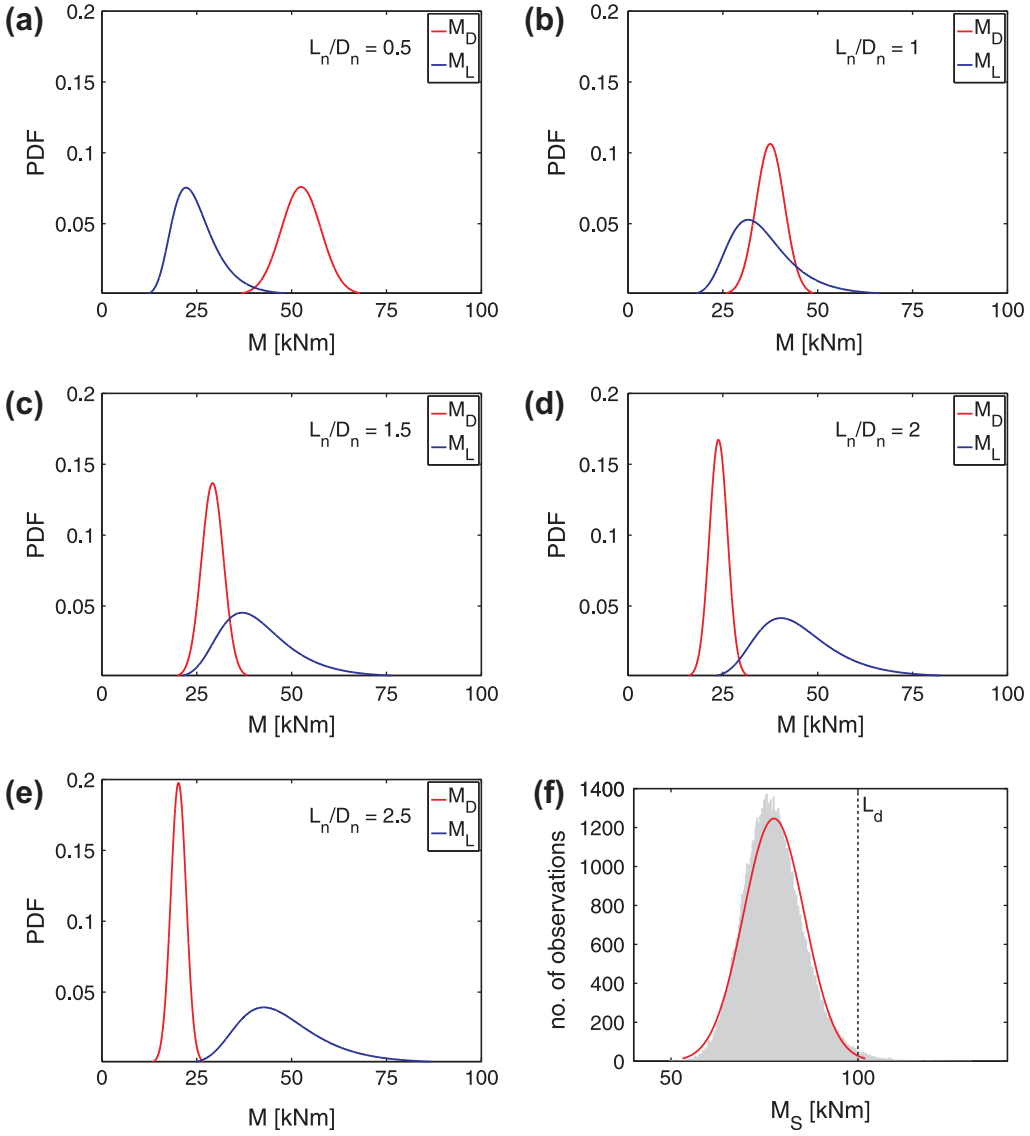

Fig. 6. (a–e) Distribution of M_L and M_D for different values of L_n/D_n ratio; i.e., 0.5, 1.0, 1.5, 2.0, 2.5 (ACI guidelines); (f) example of distribution of M_S for L_n/D_n ratio equal to 0.5 (ACI guidelines) and unsuitability of Gaussian approximation.

assessment, as also pointed out in [22]. For example, for the case where $L_n/D_n = 0.5$, using Eq. (24) and the statistics for M_R in Fig. 5b (ACI, concrete crushing), and the statistics for M_S in the first row of Table 4, β is equal to 4.5 and 4.4 with and without the Gaussian assumption for M_S, respectively. This small difference in the β values, leads to a difference in the P_f values of about 30%. For $L_n/D_n = 1$, or larger, differences of about 10% in the β values, lead to differences in P_f of an order of magnitude[6] (or larger).

Fig. 8 gives the reliability as a function of the central safety factor. In fact, even if none of the considered LRFD codes stipulates a central factor of safety, [5] recommends this format as the one of more direct interpretability. From the results it is also possible to infer the central safety factor increases as the L_n/D_n ratio increase due to the decrease of the mean of M_S (Table 4). As expected, the coefficient of variation of M_S also increases as the L_n/D_n ratios increases due to larger variability of live loads, and then β decreases with L_n/D_n.

As shown in Fig. 5, the coefficient of variation of M_R is constant for all the considered FRP codes (13%) and comparable to the coefficient of variation of M_S for low to moderate values of L_n/D_n (i.e., until 1.5); this should explain why the reliability index is of moderate sensitivity with respect to the L_n/D_n ratio (Fig. 7). This result is consistent with the study [9] referring to US guidelines where the reliability index decreases at a low rate as L_n/D_n ratio increases.

Generally, reliability indices corresponding to GFRP fracture are larger than that corresponding to concrete crushing due to the code-based conservative design formula for flexural capacity.

The assessment also indicates that ACI, when sectional failure is due to composites, is especially conservative.[7] This was expected as ACI prescribes high strength to compensate for the lack of ductility

[6] In the case of steel, given the small CoV of the M_R distribution, looking at $L_n/D_n = 2.5$, the Gaussian assumption for M_S results (considering the statistics of Fig. 5f and Table 4) in reliability index equal to about 4, while it is 3 from the more rigorous analysis.

[7] It is also to note that, failure probabilities computed herein are generally higher than what prescribed for ULS, for example, by Eurocode [4] which suggests values of β between 3.3 (ductile failure) and 4.3 (brittle failure) as minima for 50 yr as reference periods.

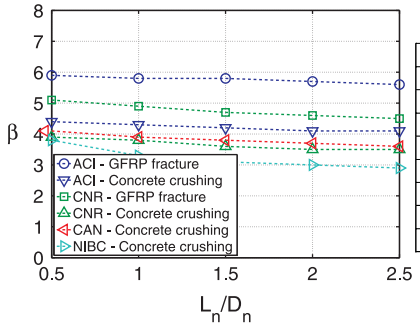

β	P_f
1	1.6×10^{-01}
2	2.3×10^{-02}
3	1.3×10^{-03}
4	3.2×10^{-05}
5	2.9×10^{-07}
6	9.9×10^{-10}
7	1.3×10^{-12}
8	6.2×10^{-16}

Fig. 7. Reliability index as a function of L_n/D_n ratio.

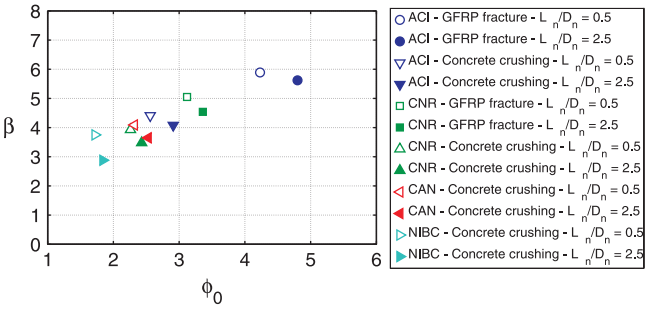

Fig. 8. Reliability indexes as a function of the central safety factor.

in the case of GFRP failure. In fact, the nominal value of bending moment of resistance is significantly reduced; e.g., by about 50%.

7.1. Sensitivity of reliability of design according to the Italian code to SF

To assess sensitivity of reliability index to safety factor of reinforcement, 490 cross sections were designed according to the Italian guidelines by varying (i) the GFRP SF between 1 and 2, with a 0.25 step, (ii) cross section width between 300 mm and 600 mm, with a step of 50 mm, (iii) cross sections height between 300 mm and 600 mm, with a step of 50 mm, and (iv) considering two relative reinforcement ratio equal to 0.5 (GFRP fracture) and 1.5 (concrete crushing), making the assessment general and covering a large number of possible design conditions.

The same procedure described above was applied to compute β, assuming a load effect ratio equal to 1. In Fig. 9a results are shown as a function of γ_f (averaging the safety indexes of the cross sections with the same value of the GFRP partial safety factor). It appears that, for the design cases corresponding to GFRP fracture, the reliability index increases at a low rate as γ_f increases (Fig. 9a), while for the design cases corresponding to concrete crushing, the reliability index is nearly constant and equal to 3.8 and then independent on the material partial safety factor. This seems consistent with the results of [8,9] and it is consistent with the design equations discussed in the previous sections, according to which, in the case of concrete crushing, M_{Rd} is independent of f_{fu} and then the influence of γ_f could be neglected.

Pilakoutas et al. [8] conclude that, provided that flexural failure occurs due to concrete crushing, the use of γ_f to account for the uncertainties in the mechanical characteristics of the FRP reinforcement is not vital, since the flexural reliability is not affected by γ_f. Based on this finding, they propose that the uncertainties relevant to mechanical characteristics of the flexural reinforcement should be incorporated into the concrete partial safety factor, eventually modifying the currently used value for it in flexural limit state design.

Finally, it is known that both mean tensile strength and its coefficient of variation vary (decreases) with the cross sectional dimensions of the bar, that is, *size-effect* (e.g., [20]). To investigate size-effect with respect to reliability, a subset of 98 cross sections of the 490 described above were considered; i.e., those corresponding to γ_f equal to 1.5.

For each case, the reliability index was computed for a load effect ratio equal to 1 by varying the bar size between #2 (i.e., diameter equal to 6 mm) and #10 (i.e., diameter equal to 32 mm). Statistics reported in [26], which change as a function of the size, were used for the reliability assessment.

For the design cases corresponding to GFRP fracture, all the indexes were plotted in Fig. 9b as a function of bar size showing that the reliability index is almost constant. Same trends, yet smaller values of reliability index (i.e., about 3.9), have been found in the case of concrete crushing.

Analyses indicate that bar size appears to be not important with respect to reliability; however, FRP reinforcing bars with large dimensions may affect the bonding with concrete.

8. Conclusions

Currently, noncorrosive and nonconductive FRP bars are emerging as an alternative to conventional steel reinforcement for structural concrete. In this paper, the *conventional* reliability (meaning that failure probabilities are to be taken for comparative purposes only and may not be interpreted as actual failure probabilities) implied by design of FRP-reinforced sections in bending was investigated.

ACI 440.1R-06 guidelines, CAN/CSA-S806-02 guidelines, and the Italian guidelines CNR-DT 203/2006 were compared, with the aim of investigating how the different design procedures and formats affect the implicit design safety and whether it is similar among international guidelines. As a benchmark, the design of steel-reinforced concrete cross sections, according to the recent Italian code, was also considered.

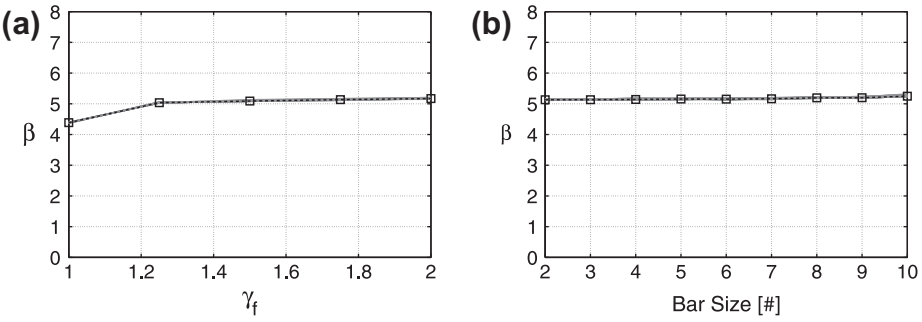

Fig. 9. (a) Reliability index as a function γ_f for case study cross sections governed by GFRP fracture; (b) reliability index as a function of the bars' diameter for case study cross sections governed by GFRP fracture.

The study focused exclusively on the flexural behavior of GFRP-RC sections. It was found that, although design formats are quite different, codes lead to generally comparable reliability indices (which, however, have an exponential link with the probability of failure) among codes and relatively high with respect to concrete reinforced with steel. ACI may be relatively conservative when sectional failure is due to FRP.

The parametric study for the Italian guidelines, indicates that for the design cases corresponding to GFRP fracture, the reliability index increases at a low rate as γ_f increase, while for the design cases corresponding to concrete crushing, as found in other similar studies, the conservative partial safety factor for FRP reinforcement has little influence on the safety of cross sections.

The issue of size-effect in FRP strength was also investigated in the structural reliability framework; analyses seem to suggest that bar size appears to be not important with respect to reliability, although, FRP reinforcing bars with large dimensions may affect the bonding with concrete.

Acknowledgement

The authors want to thank Racquel K. Hagen of Stanford University for proofreading the manuscript.

References

[1] Ellingwood BE, MacGregor JG, Galambos TV, Cornell CA. Probability-based load criteria: load factors and load combinations. J Struct Div, ASCE 1982;108(5):978–97.
[2] Benjamin JR, Cornell CA. Probability, statistics and decision for civil engineers. New York: McGraw-Hill; 1970.
[3] Pinto PE, Giannini R, Franchin P. Seismic reliability of structures. Pavia, Italy: IUSS Press; 2004, ISBN 88-7358-017-3.
[4] CEN, European Committee for Standardisation (CEN). Eurocode: basis of strucutral desing, EN 1990; 2002.
[5] Cornell CA. A probability-based structural code. ACI Struct J 1969;66(12):974–85.
[6] Cornell CA. Probability bases for structural design. In: Ghiocel D, Lungu D, editors. Wind snow and temperature effects on structures based on probability. UK: Abacus Press; 1976.
[7] Monti G, Santini S. Reliability-based calibration of partial safety coefficients for fiber-reinforced plastic. J Compos Constr 2002;6(3):162–7.
[8] Pilakoutas K, Neocleous K, Guadagnini M. Design philosophy issues of fiber reinfored polymer reinforced concrete structures. J Compos Constr 2002;6(3):154–61.
[9] He Z, Qiu F. Probabilistic assessment on flexural capacity of GFRP-reinforced concrete beams designed by guideline ACI 440.1R-06. Constr Build Mater 2010;25(4):1663–70.
[10] American Concrete Institute (ACI) Committee 440. ACI 440.1R-06: Guide for the design and construction of structural concrete reinforced with FRP bars; 2006.
[11] Canadian Standards Association (CSA). CSA-S806-02: Design and construction of building components with fibre-reinforced polymers; 2002.
[12] Consiglio Nazionale delle Ricerche (CNR). CNR-DT 203/2006: Guide for the design and construction of concrete structures reinforced with fiber-reinforced polymer bars; 2006.
[13] CS.LL.PP. Decreto Ministeriale 14 Gennaio 2008: Norme tecniche per le costruzioni. Gazzetta Ufficiale della Repubblica Italiana, no. 29, 4 febbraio 2008, Suppl. Ordinario no. 30; 2008 [in Italian].
[14] Ellingwood B, Galambos TV, MacGregor JG, Cornell CA. Development of a probability based load criterion for American national standard A58 building code requirements for minimum design loads in buildings and other structures, Special Publication 577. Washington (DC, USA): US Department of Commerce, National Bureau of Standards; 1980.
[15] Cosenza E, Iervolino I. Case study: seismic retrofitting of a medieval bell tower by FRP. J Compos Constr 2007;11(3):319–27.
[16] Pecce M, Manfredi G, Cosenza E. Experimental response and code models of GFRP RC beams in bending. J Compos Constr 2000;4(4):182–90.
[17] Nanni A. North American design guidelines for concrete reinforcement and strengthening using FRP: principles, applications and unresolved issues. Constr Build Mater 2003;17(6–7):439–46.
[18] American Concrete Institute (ACI) Committee 318, 20022005. ACI 318-0205: Building code requirements for structural concrete and commentary.
[19] Consiglio Nazionale delle Ricerche (CNR). CNR-DT 200/2004: Guide for the design and construction of externally bonded FRP systems for strengthening existing structure; 2004.
[20] Kocaoz S, Samaranayake VA, Nanni A. Tensile characterization of glass FRP bars. Compos B Eng 2005;36(2):127–34.
[21] Nowak AS, Szerszen MM. Calibration of design code, for buildings (ACI318): Part 1 – statistical models for resistance. ACI Struct J 2003;100(3):377–82.
[22] Zureick AH, Bennett RM, Ellingwood BR. Statistical characterization of FRP composite material properties for structural design. J Struct Eng 2006;132(8):1320–7.
[23] Gumbel EJ. Probabilistic analysis of loads. In: Ghiocel D, Lungu D, editors. Wind snow and temperature effects on structures based on probability. UK: Abacus Press; 1976.
[24] Fico R. Limit states design of concrete structures reinforced with FRP bars. PhD thesis, Univ. of Naples, Italy; 2007. p. 167.
[25] Mood MA, Graybill FA, Boes DC. Introduction to the theory of statistics. 2nd ed. New York: McGraw-Hill; 1974.
[26] Kulkarni S. Calibration of flexural design of concrete members reinforced with FRP bars. MSc Thesis, Louisiana State University and Agricultural and Mechanical College; 2006.